Pilot Assignment for Cell-Free Systems Serving Ground Users and Unmanned Aerial Vehicles

Maria Clara R. Lobão, Wilker de O. Feitosa, Roberto P. Antonioli,
Iran M. Braga Jr., Yuri C. B. Silva, Walter C. Freitas Jr., Gábor Fodor

Abstract—This study evaluates the performance of cell-free massive multiple input multiple output systems serving Unmanned aerial vehicles (UAVs) subject to Rician fading channels. The studied cell-free systems can be implemented employing three different levels of cooperation between the access points, namely: level 3, which is a fully centralized approach; level 2, which is a partially centralized approach with large-scale fading decoding weights; and level 1, which is a fully decentralized approach resembling small-cell systems. We study the performance of five different pilot assignment methods, while considering a mix of served UAVs and ground user equipments. The results show how the presence of UAVs with good propagation conditions impacts the overall performance in terms of the achieved spectral efficiency. Specifically, our results show that one of the pilot assignment algorithms provides the best trade-off between the spectral efficiencies allocated to UAVs and ground users.

Keywords— Cell-free massive MIMO, levels of centralization, pilot assignment, UAV communications.

I. INTRODUCTION

The studies of cell-free massive multiple input multiple output (MIMO) networks indicate that these systems are most efficient when serving a large numbers of users and intense data traffic [1]. Specifically, cell-free systems can achieve high resource utilization and superior per-user performance over the entire coverage area of the system due to the cell-free design and large-scale spatial multiplexing.

Connected Unmanned aerial vehicles (UAVs), or drones, are of increasing interest in a number of transport segments, including urban air mobility, goods delivery, industrial surveillance and environmental monitoring. Employing connected drones in such applications are attractive, since they offer a low-cost and convenient alternative to costly traditional solutions relying on ground transportation and fixed infrastructures [2]. Thus, herein we focus on how cell-free systems serving UAVs subject to Rician fading channels perform, while considering a probability of having line of sight (LOS) components.

Pilot transmission is an important stage of the data processing in MIMO systems, enabling channel state information (CSI) estimation and, hence, enabling efficient channel-adaptive transmission schemes. However, the limited number of orthogonal pilot sequences in the system induces the reuse of these signals between multiple user equipments (UEs), increasing interference and causing pilot contamination, which results in imperfect channel estimation and degraded service quality for the UEs. Recognizing the importance of pilot assignments, in this study we study the performance of different pilot management schemes specifically in cell-free systems.

One of the issues of implementing pilot assignment methods in a cell-free system is related to their computational complexity. As mentioned in [3], the complexity of pilot assignment algorithms increases exponentially as the number of UEs in the system grows, resulting in a non-polynomial time (NP)-hard problem. The pilot assignment schemes studied in this work are non-optimal algorithms, implemented in a distributed fashion, such as the random [3] and scalable [4] pilot assignment solutions, or in a centralized manner, such as the greedy [5] and random sequential adsorption (RSA) [3] pilot assignments.

In cell-free systems with UAVs, the pilot interference between UAVs and ground user equipments (GUEs) is strong, which degrades the quality of service of the GUEs. Thus, pilot assignment plays a central role in improving the rate achieved by all UEs. The random and RSA pilot assignment solutions offer the simplest implementation, since the first method does not require any parameter to perform the allocation, while the second method requires only the UEs' positions as input parameters for the assignment. Neither of these algorithms, however, guarantees the reduction of pilot contamination between UAVs and GUEs. Both the greedy and scalable pilot assignments seek reducing the pilot interference among the users, taking into account the correlation of the received signal at the access point (AP). However, the greedy solution takes into consideration the uplink rate of all the UEs in the system, increasing its complexity. Since greedy and scalable pilot assignment solutions perform interference minimization, the pilot reuse between UAV and GUE is also reduced.

In this work, we evaluate the performance of cell-free massive MIMO systems with different levels of cooperation between the APs, as developed in [6], while considering different propagation and path-loss models as well as UAVs and GUEs. The results are obtained via analyzing the cumulative distribution function (CDF) of the uplink spectral efficiency

(SE) of each scenario for both UAVs and GUEs. The results show that the UAVs' better propagation conditions increase the interference upon the GUEs, impacting their performance negatively. Furthermore, it is shown that the scalable pilot assignment algorithm provides the best trade-off between the spectral efficiencies allocated to UAVs and ground users.

II. SYSTEM MODEL

We consider a cell-free massive MIMO network consisting of L APs, each one equipped with N antennas, K_{UAV} UAVs and K_{GUE} GUEs. The total number of UEs in the system is denoted by $K = K_{\text{UAV}} + K_{\text{GUE}}$. All UEs are equipped with a single antenna. The APs are connected via fronthaul links to a central processing unit (CPU). The system employs time division duplex (TDD) and an uplink (UL) operation is considered.

A. Propagation Model

The propagation channels between the k-th UE and the l-th AP, denoted by $\mathbf{h}_{k,l} \in \mathbb{C}^N$, follow a Rician fading model [2], with LOS and non-line of sight (NLOS) components, and is described as follows:

$$\mathbf{h}_{k,l} = \left[\sqrt{\frac{\bar{K}_{k,l}}{\bar{K}_{k,l}+1}} \mathbf{a}_{k,l}\left(\theta_{k,l}\right) + \sqrt{\frac{1}{\bar{K}_{k,l}+1}} \mathbf{h}_{k,l}^{(w)} \right] \sqrt{\beta_{k,l}}, \tag{1}$$

in which $\mathbf{h}_{k,l}^{(w)} \sim \mathcal{N}(0, \mathbf{R}_{k,l})$ is the NLOS Rayleigh fading component with $\mathbf{R}_{k,l}$ being the spatial correlation matrix, describing the channel's spatial characteristics, $\beta_{k,l}$ is the large scale coefficient modeling the path-loss and shadowing gains, and $\bar{K}_{k,l}$ is the Rician K-factor. The term $\mathbf{a}_{k,l}\left(\theta_{k,l}\right)$ represents the steering vector between the UE and the linear array of antennas on the AP [7] and is modeled as:

$$\mathbf{a}_{k,l}\left(\theta_{k,l}\right) = \left[a_1, \ldots, a_N\right]^T. \tag{2}$$

For the n-th antenna, a_n is modeled with the phase-shifts, and can be described by the expression:

$$a_n = e^{-j\frac{2\pi}{\lambda} d \sin \theta_{k,l}}, \tag{3}$$

where d represents the spacing between the antennas, λ is the wavelength, and $\theta_{k,l}$ is the angle of arrival of the signal from the k-th UE to the l-th AP.

In this model, both the UAVs and the GUEs are associated with a LOS probability, while the channel characteristics are determined by the horizontal distance (d_{2D}), in meters, between the UE and the AP. For the UAVs, the LOS probability is given by the expression:

$$P_{\text{LOS}} = \begin{cases} 1, & d_{\text{2D}} \leq d_1, \\ \dfrac{d_1}{d_{\text{2D}}} + \exp\left(-\dfrac{d_{\text{2D}}}{p_1}\right)\left(1 - \dfrac{d_1}{d_{\text{2D}}}\right), & d_{\text{2D}} > d_1, \end{cases} \tag{4}$$

in which d_1 and p_1 are positive constants given by the expressions in [8], which relate the LOS probability with the UAV heights, and vary in the considered scenarios.

For the GUEs, the LOS probability is:

$$P_{\text{LOS}} = \begin{cases} 1, & d_{\text{2D}} \leq 18m, \\ \dfrac{18}{d_{\text{2D}}} + \exp\left(-\dfrac{d_{\text{2D}}}{36}\right)\left(1 - \dfrac{18}{d_{\text{2D}}}\right), & d_{\text{2D}} > 18m. \end{cases} \tag{5}$$

Given the LOS probabilities, we can determine the Rician K-Factor $\bar{K}_{k,l}$ between the l-th AP and the k-th UE. If the channel is LOS, $\bar{K}_{k,l}$ is 15dB for UAVs and $\mathcal{N}(9,5)$dB for GUEs; if the channel of the UE k is NLOS, $\bar{K}_{k,l}$ will be 0, according to [8] and [9], for the urban micro (UMi) scenario.

The large-scale coefficient $\beta_{k,l}$ is described as:

$$\beta_{k,l} = 10^{\frac{PL_{k,l}+SH_{k,l}}{10}}, \tag{6}$$

in which $PL_{k,l}$ is the path-loss gain in dB, modeled following the specifications in [8] and [9] for UAVs and GUEs, respectively, and $SH_{k,l}$ represents the correlated shadowing, described by the standard deviation σ_{sh}.

B. Channel Estimation

As described in [6], the channel is estimated based on pilot transmission. We assume $\tau_p < K$ orthogonal τ_p-length pilot signals $\phi_1, \ldots, \phi_{\tau_p}$, with $\| \phi_t \|^2 = \tau_p$. Utilizing the pilots transmitted by the users, the AP correlates the normalized pilot with the received signal, obtaining $z_{k,l}$, given by:

$$\mathbf{z}_{t_k,l} = \sum_{i \in \mathcal{P}_k} \sqrt{p_i \tau_p} \mathbf{h}_{i,l} + \mathbf{n}_{t_k,l}, \tag{7}$$

where p_i is the transmit power of UE i, $\mathcal{P}_k$ is the set of users that use the same pilot as UE k, t_k is the index of the pilot used by UE k, and $\mathbf{n}_{t_k,l} \sim \mathcal{N}(0, \sigma^2 \mathbf{I}_N)$. Then, the AP estimates the channel using minimum mean square error (MMSE) estimation[1]:

$$\hat{\mathbf{h}}_{k,l} = \sqrt{p_k \tau_p} \mathbf{R}_{k,l} \boldsymbol{\Psi}_{t_k,l}^{-1} \mathbf{z}_{t_k,l}, \tag{8}$$

in which $\boldsymbol{\Psi}_{t_k,l} = \mathbb{E}\{\mathbf{z}_{t_k,l}\mathbf{z}_{t_k,l}^H\}$. The estimation error is given by $\tilde{\mathbf{h}}_{k,l} = \mathbf{h}_{k,l} - \hat{\mathbf{h}}_{k,l}$.

In the next section, we describe the pilot assignment schemes that we study in this paper.

III. PILOT ASSIGNMENT METHODS

We consider five different methods of pilot assignment in this study: random assignment, RSA-based assignment, greedy assignment, assignment for scalable systems and cluster formation [4], and a pilot assignment that separates the pilots used by GUEs and UAVs.

A. Random Pilot Assignment

In this method, the τ_p orthogonal pilot signals are assigned to each UE randomly. Given that the number of pilots is limited to $\tau_p < K$, we have that some of the users will share the same pilot; moreover, considering that the UEs will be assigned a pilot without any regulation, users in close proximity might share the same pilot signal, which increases the pilot contamination.

---

[1]Note that performance can be improved when using MMSE receivers specifically designed to account for CSI errors, such as in [10].

B. RSA-based Pilot Assignment

This pilot assignment method was proposed in [3]. The RSA process consists of introducing elements into a system randomly and fixing them if they don't overlap with any other element previously fixed.

The pilot allocation algorithm based on this process considers a circle of radius r centered at the k-th UE. The UE is first assigned a pilot randomly; then, the algorithm checks if any other UE under the radius r is using the same pilot signal. If it is not being used, then the pilot is attributed to the UE k; otherwise, the UE is assigned another pilot randomly and the process repeats. This method is implemented using a confined number of iterations, to guarantee the feasibility and convergence of the algorithm assuming realistic channel coherence times.

C. Scalable Pilot Assignment

In this algorithm, proposed in [4], each UE selects as its Master AP the one with the best large scale coefficient $\beta_{k,l}$:

$$l = \arg \max_l \beta_{k,l} . \qquad (9)$$

The appointed AP will perform the data reception. After all the τ_p pilots have already been allocated, the Master AP will, then, search for the pilot ϕ_τ that presents the least pilot contamination, computed using the correlation matrix of the received signal $\mathbf{\Psi_{t_k,l}}$:

$$\tau = \arg \min_{t_k} \mathrm{tr} \left(\mathbf{\Psi}_{t_k,l} \right) . \qquad (10)$$

The pilot τ is assigned to the UE k. This process is repeated for every UE, but done only considering its Master AP.

D. Greedy Pilot Assignment Algorithm

In this method, all UEs in the system are assigned a pilot sequence randomly. Then, the UE with the lowest uplink rate, considering the rate expression given in [5], is selected to modify its pilot signal in order to decrease pilot interference.

Given the UE k with the lowest rate, its pilot sequence is updated by choosing the pilot ϕ_{t_k} which minimizes:

$$\arg \min_{\phi_{t_k}} \sum_{l=1}^{L} \sum_{k' \neq k}^{K} \beta_{l,k'} \left| \phi_{t_{k'}}^H \phi_{t_k} \right|^2 . \qquad (11)$$

Knowing that the pilots are mutually orthogonal, we have that $\left| \phi_{t_{k'}}^H \phi_{t_k} \right|^2 = 0$ if $t_{k'} \neq t_k$. If $t_{k'} = t_k$, then $\left| \phi_{t_{k'}}^H \phi_{t_k} \right|^2 = \tau_p$. Hence, considering $\mathcal{P}_{t_k}$ as the set of UEs that share the same pilot, except for UE k, we can rewrite (11) as:

$$\arg \min_{\phi_{t_k}} \sum_{l=1}^{L} \sum_{k' \in \mathcal{P}_{t_k}} \beta_{l,k'} \tau_p . \qquad (12)$$

Similarly to the RSA pilot assignment, this algorithm has to be performed using a limited number of iterations.

E. Pilot Assignment with Reservation Scheme

Due to the best propagation conditions in comparison to the GUEs, the UAVs of the system induce high pilot interference if they share the same pilot with a GUE, and, consequently, decrease their efficiency.

In this solution, as described in [11], we separate a set of the pilots to serve only the UAVs, and the remaining ones serve only the GUEs. With this scheme, we avoid pilot contamination between the UAVs and GUEs, but it is still necessary to minimize the pilot contamination in each case. In order to analyze whether there are benefits in terms of SE for the UAVs, we consider only a simple random pilot assignment, described in section III-A, and for the GUEs, we perform pilot decontamination using the scalable pilot assignment, as described in section III-C.

IV. LEVELS OF CENTRALIZATION

As mentioned in section II, the APs of the cell-free system are connected to a CPU. The interaction between these elements affects the behavior of the system. In this context, the UL training can be done in four different levels of cooperation among APs.

The adopted modeling of the cell-free system, as well as the computation of the SE, is done based on the work in [6]. Considering the performance presented by each level, we chose to evaluate the ones with the best results, levels 3 and 2, and also level 1, which is the representation of a small-cell system[2]. The scenarios are summarized as follows:

Level 3: This is the maximum level of centralization, in which the APs send the received pilot sequences and data to the CPU, which is responsible for the signal processing and channel estimation. The achievable SE of user k in this level is calculated as follows:

$$\mathrm{SE}_k^{(3)} = \left(1 - \frac{\tau_p}{\tau_c} \right) \mathbb{E} \left\{ \log_2 \left(1 + \gamma_k^{(3)} \right) \right\} , \qquad (13)$$

where τ_c is the length of the coherence time and $\gamma_k^{(3)}$ is the maximum instantaneous signal to interference-plus-noise ratio (SINR)[3], given the instantaneous estimated channels $\hat{\mathbf{h}}_k$. Assuming that $\hat{\mathbf{h}}_k \triangleq [\hat{\mathbf{h}}_{k,1} \cdots \hat{\mathbf{h}}_{k,L}]^T$, $\gamma_k^{(3)}$ can be written as [6]:

$$\gamma_k^{(3)} = p_k \hat{\mathbf{h}}_k^H \left(\sum_{i=1,i\neq k}^{K} p_i \hat{\mathbf{h}}_i \hat{\mathbf{h}}_i^H + \sum_{i=1}^{K} p_i \mathbf{C}_i + \sigma^2 \mathbf{I}_{LN} \right)^{-1} \hat{\mathbf{h}}_k, \qquad (14)$$

in which the expectation in (13) is taken over $\hat{\mathbf{h}}_k$; $\gamma_k^{(3)}$ is maximized using the MMSE combining vector:

$$\mathbf{v}_k = p_k \left(\sum_{i=1}^{K} p_i \left(\hat{\mathbf{h}}_i \hat{\mathbf{h}}_i^H + \mathbf{C}_i \right) + \sigma^2 \mathbf{I}_{LN} \right)^{-1} \hat{\mathbf{h}}_k, \qquad (15)$$

with $\mathbf{C}_k = \mathrm{diag}(\mathbf{C}_{k,1}, \ldots, \mathbf{C}_{k,L})$ and $\mathbf{C}_{k,l} = \mathbb{E}\{\tilde{\mathbf{h}}_{k,l}\tilde{\mathbf{h}}_{k,l}^H\}$.

---

[2]The level 3 considered in our work corresponds to the level 4 from [6], our level 2 corresponds to the level 3 from [6], and the level 1 is equal to the level 1 from [6].

[3]The maximum achievable SINR assuming only the desired signal over the estimated channel [12].

Level 2: This is a partially centralized scenario. In this level, the AP performs the channel estimation, then sends the collected data do the CPU, which executes the decoding using large scale fading decoding (LSFD) weights, denoted by $\mathbf{w}_k$. If this level is implemented in an optimal manner, then the LSFD weights will be computed as to maximize the SINR [12]:

$$\mathbf{w}_k = \left(\sum_{i=1}^{K} p_i \mathbb{E}\{\mathbf{g}_{k,i}\mathbf{g}_{k,i}^H\} + \sigma^2 \mathbf{D}_k \right)^{-1} \mathbb{E}\{\mathbf{g}_{k,k}\}, \quad (16)$$

with $\mathbf{D}_k = \text{diag}\left(\mathbb{E}\{||\mathbf{v}_{k,1}||^2\} \ldots \mathbb{E}\{||\mathbf{v}_{k,L}||^2\} \right) \in \mathbb{C}^{L \times L}$, $\mathbf{g}_{k,i} = \left[\mathbf{v}_{k,1}^H \mathbf{h}_{i,1} \ldots \mathbf{v}_{k,L}^H \mathbf{h}_{i,L} \right]^T$ and $\mathbf{v}_{k,l}$ representing the MMSE combining vector, given by:

$$\mathbf{v}_{k,l} = p_k \left(\sum_{i=1}^{K} p_i \left(\hat{\mathbf{h}}_{i,l} \hat{\mathbf{h}}_{i,l}^H + \mathbf{C}_{i,l} \right) + \sigma^2 \mathbf{I}_N \right)^{-1} \hat{\mathbf{h}}_{k,l}. \quad (17)$$

The achievable SE is expressed as:

$$\text{SE}_k^{(2)} = \left(1 - \frac{\tau_p}{\tau_c} \right) \log_2 \left(1 + \text{SINR}_k^{(2)} \right), \quad (18)$$

where $\text{SINR}_k^{(2)}$ is the maximum SINR value obtained using (16), given by [6]:

$$\text{SINR}_k^{(2)} = p_k \mathbb{E}\{\mathbf{g}_{k,k}^H\} \left(\sum_{i=1}^{K} p_i \mathbb{E}\{\mathbf{g}_{k,i}\mathbf{g}_{k,i}^H\} + \sigma^2 \mathbf{D}_k \right.$$
$$\left. - p_k \mathbb{E}\{\mathbf{g}_{k,k}\}\mathbb{E}\{\mathbf{g}_{k,k}^H\} \right)^{-1} \mathbb{E}\{\mathbf{g}_{k,k}\}. \quad (19)$$

Level 1: This is the most distributed scenario, in which the entire processing, channel estimates and decoding is done at the AP, characterizing this level as a small-cells network. The achievable SE of UE k is given by:

$$\text{SE}_k^{(1)} = \left(1 - \frac{\tau_p}{\tau_c} \right) \max_{l \in \{1,...,L\}} \mathbb{E}\left\{ \log_2 \left(1 + \gamma_{k,l}^{(1)} \right) \right\}, \quad (20)$$

with the expectation taken over the channel estimates. The maximum value of the SINR $\gamma_{k,l}^{(1)}$ is obtained using the combining vector (17) and is given by [6]:

$$\gamma_{k,l}^{(1)} = p_k \hat{\mathbf{h}}_{k,l}^H \left(\sum_{i=1,i\neq k}^{K} p_i \hat{\mathbf{h}}_{i,l} \hat{\mathbf{h}}_{i,l}^H + \sum_{i=1}^{K} p_i \mathbf{C}_{i,l} + \sigma^2 \mathbf{I}_N \right)^{-1} \hat{\mathbf{h}}_{k,l}. \quad (21)$$

V. SIMULATION AND RESULTS

The cell-free massive MIMO scenarios were simulated using Python3 and the results were obtained in terms of the CDF of the UL SE of the users in 200 setups, separating the performances of the UAVs and the GUEs. For each setup, the SINR of each user is averaged over 200 channel realizations and the respective SE is calculated.

We consider each setup consisting of $K = 40$ UEs randomly located within the square coverage area of 1 km², in which $K_{\text{UAV}} = 16$ and $K_{\text{GUE}} = 24$. There were $L = 100$ APs, each equipped with a linear array of $N = 4$ antennas. The pilot

signals were assumed to be transmitted with full power and the parameters for the channel modeling and the SE computation are given in Table I, with h_{GUE}, h_{UAV} and h_{AP} representing the GUE, UAV and AP heights, respectively.

TABLE I
SIMULATION PARAMETERS.

Carrier frequency	f_c = 2 GHz
Communication bandwidth	W = 20 MHz
h_{GUE}, h_{AP}	1.5 m, 11.5 m
h_{UAV}	uniform, $[23, 230]$ m
UL power per UE	p_k = 100 mW
Antenna spacing	$d = (1/2)\lambda$
Number of pilots	$\tau_p = 10$
Coherence block length	$\tau_c = 200$
GUEs σ_{sh} (LOS, NLOS)	4, 8.2
UAVs σ_{sh} (LOS [8], NLOS)	$\max(2, 5e^{h_{\text{UAV}}/100})$, 8

The system performance is analyzed considering the levels of centralization from Section IV and the pilot assignment algorithms presented in Section III.

A. Centralization Levels Analysis

Figure 1 shows the results of the three levels of cooperation for the scalable pilot assignment. As expected from the results in [6], the highest level of centralization achieved the best values of SE, for both the UAVs and GUEs, unlike the other levels, which presented a large performance gap compared to level 3, with the level 1 presenting the lowest values.

The UAVs present in the system achieved a better performance in comparison to the GUEs, due to their best
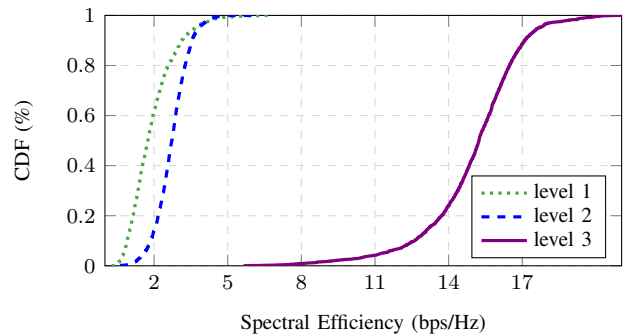
(a) UAV results.
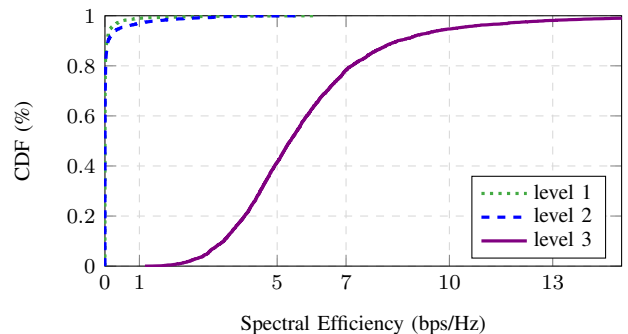
(b) GUE results.

Fig. 1. Spectral Efficiency for UAVs and GUEs, comparing the 3 levels of cooperation, $N = 4$ and $L = 100$.

propagation conditions, and their CDF curves reflect this behavior. The LOS and NLOS components of the UEs also have a considerable influence on the SE quality, since the large number of APs contributes to better LOS components to the UAVs. In the simulations, we have that the UAVs presented around 83% of LOS cases, while the GUEs showed around 0.8% of LOS cases, considering that the same UE might have LOS and NLOS propagation conditions for different APs.

Given that the GUEs are affected by the UAVs stronger channels, their performance decreases, as it can be noticed by the curves of levels 2 and 1 in Figure 1b. Note that these same centralization levels achieve the worst performances for the UAVs as well, as already shown in Figure 1a. For these distributed scenarios, the interference at the AP is much higher for the GUEs than for the UAVs, which in the case of level 2, also affects the computation of the LSFD weights, degrading the overall results.

B. Pilot Assignment Analysis

Figure 2a shows the performance obtained by each pilot assignment method for the UAVs. All methods present very similar performances, with the random assignment method performing slightly worse than the others.

The RSA and the greedy methods presented close results. In both of these algorithms the assignment can be understood as a random pilot allocation that is optimized. Specifically, the former considers a minimum distance of $r = 100$ m to perform pilot reuse, while the latter updates the pilot allocation of the worst UE in 100 iterations. Hence, as in both cases the

pilot reuse is minimized, their performances are better than the random pilot assignment. As observed in Figure 2b, these three algorithms also give similar results, with the advantage of the RSA performing best with a considerably lower computational complexity. Due to the worse propagation conditions, the worst UEs in the greedy algorithm are always the GUEs; with a higher number of iterations, their performance using this method can be improved.

The scalable pilot assignment showed a satisfactory performance, achieving the best trade-off for UAVs and GUEs, since for every UE the algorithm looks for the pilot presenting the least contamination at the master AP. In the reservation scheme, since there is a pool of pilots restricted for UAVs, the pilot contamination is decreased for them, as seen in Figure 2a, but as a consequence the GUEs are negatively affected and present by far the worst performance with this scheme.

VI. CONCLUSION

In this study, we evaluated the performance of cell-free massive MIMO systems with different levels of AP cooperation, considering a scenario with UAVs and GUEs, in which both have LOS and NLOS conditions. We observed that the presence of the UAVs in the system resulted in a considerable decrease in the performance of the GUEs, which can be explained by their better propagation conditions and LOS components. The impact of different pilot assignment algorithms was also analyzed, in which we observed how each allocation method contributed to diminish the pilot contamination among UEs, specially between UAVs and GUEs, since the former have better channels that lead to stronger contamination.

REFERENCES

[1] S. Chen, J. Zhang, J. Zhang, E. Björnson, and B. Ai, "A survey on user-centric cell-free massive MIMO systems," *Digital Communications and Networks*, Dec. 2021. DOI: 10.1016/j.dcan.2021.12.005.

[2] C. D'Andrea, A. Garcia-Rodriguez, G. Geraci, L. G. Giordano, and S. Buzzi, "Cell-free massive MIMO for UAV communications," in *Proc. IEEE Int. Conf. on Commun. Workshops (ICC)*, May 2019, pp. 1–6.

[3] P. Parida and H. S. Dhillon, *Pilot assignment schemes for cell-free massive MIMO systems*, 2021. [Online]. Available: https://arxiv.org/abs/2105.09505.

[4] E. Björnson and L. Sanguinetti, "Scalable cell-free massive MIMO systems," *IEEE Trans. Commun.*, vol. 68, no. 7, pp. 4247–4261, Jul. 2020. DOI: 10.1109/tcomm.2020.2987311.

[5] H. Q. Ngo, A. Ashikhmin, H. Yang, E. G. Larsson, and T. L. Marzetta, "Cell-free massive MIMO versus small cells," *IEEE Trans. Wireless Commun.*, vol. 16, no. 3, pp. 1834–1850, Jan. 2017.

[6] E. Björnson and L. Sanguinetti, "Making cell-free massive MIMO competitive with MMSE processing and centralized implementation," *IEEE Trans. Wireless Commun.*, vol. 19, no. 1, pp. 77–90, Sep. 2019.

[7] S. R. Saunders and S. R. Simon, *Antennas and Propagation for Wireless Communication Systems*, 1st. John Wiley & Sons, 1999.

[8] 3GPP, "Enhanced LTE support for aerial vehicles," TR 36.777, Jan. 2018, v.15.0.0.

[9] 3GPP, "Study on channel model for frequencies from 0.5 to 100 GHz," TR 38.901, Mar. 2022, v.17.0.0.

[10] A. Abrardo, G. Fodor, M. Moretti, and M. Telek, "MMSE receiver design and SINR calculation in MU-MIMO systems with imperfect CSI," *IEEE Wireless Communications Letters*, vol. 8, no. 1, pp. 269–272, Feb. 2019. DOI: 10.1109/LWC.2018.2869763.

[11] G. Geraci, A. Garcia-Rodriguez, L. Galati Giordano, D. López-Pérez, and E. Björnson, "Understanding UAV cellular communications: From existing networks to massive MIMO," *IEEE Access*, vol. 6, pp. 67853–67865, 2018. DOI: 10.1109/ACCESS.2018.2876700.

[12] Ö. T. Demir, E. Björnson, and L. Sanguinetti, "Foundations of user-centric cell-free massive MIMO," *Foundations and Trends in Signal Processing*, vol. 14, no. 3-4, pp. 162–472, 2021.
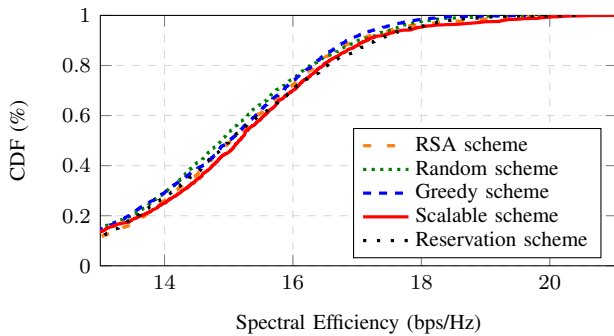
(a) UAV results.
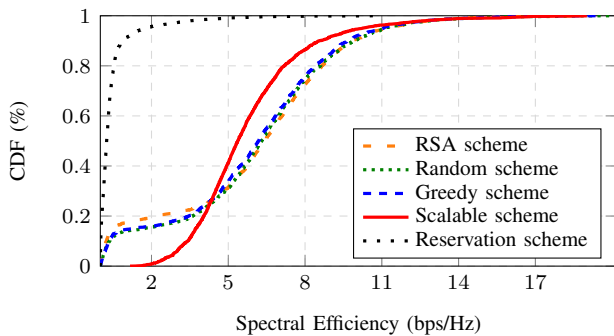
(b) GUE results.

Fig. 2. Spectral Efficiency for UAVs and GUEs, both using the 3rd level of cooperation, $N = 4$ and $L = 100$.